Petroleum Science 21 (2024) 244–251

Contents lists available at ScienceDirect

Petroleum Science

journal homepage: www.keaipublishing.com/en/journals/petroleum-science

Original Paper

# A novel algorithm for evaluating cement azimuthal density based on perturbation theory in horizontal well

Ji-Lin Fan [a, b], Feng Zhang [a, *], Qian Chen [c], Hao-Chen Song [b], Lu-Yu Zhong [a], Yue-Xiang Dai [b]

[a] *National Key Laboratory of Deep Oil and Gas, School of Geosciences, China University of Petroleum (East China), Qingdao 266580, Shandong, China*
[b] *China National Logging Corporation, Xi'an 710076, Shaanxi, China*
[c] *Sinopec Matrix Corporation, Qingdao 266001, Shandong, China*

A R T I C L E I N F O

*Article history:*
Received 11 May 2022
Received in revised form
20 July 2023
Accepted 10 October 2023
Available online 11 October 2023

Edited by Jie Hao and Meng-Jiao Zhou

*Keywords:*
Cement azimuthal density
Perturbation theory
Casing eccentricity
Spatial dynamic response function
Regularized Newton iteration

A B S T R A C T

Cement density monitoring plays a vital role in evaluating the quality of cementing projects, which is of great significance to the development of oil and gas. However, the presence of inhomogeneous cement distribution and casing eccentricity in horizontal wells often complicates the accurate evaluation of cement azimuthal density. In this regard, this paper proposes an algorithm to calculate the cement azimuthal density in horizontal wells using a multi-detector gamma-ray detection system. The spatial dynamic response functions are simulated to obtain the influence of cement density on gamma-ray counts by the perturbation theory, and the contribution of cement density in six sectors to the gamma-ray recorded by different detectors is obtained by integrating the spatial dynamic response functions. Combined with the relationship between gamma-ray counts and cement density, a multi-parameter calculation equation system is established, and the regularized Newton iteration method is employed to invert casing eccentricity and cement azimuthal density. This approach ensures the stability of the inversion process while simultaneously achieving an accuracy of 0.05 g/cm$^3$ for the cement azimuthal density. This accuracy level is ten times higher compared to density accuracy calculated using calibration equations. Overall, this algorithm enhances the accuracy of cement azimuthal density evaluation, provides valuable technical support for the monitoring of cement azimuthal density in the oil and gas industry.


## 1. Introduction

Cementing engineering is of great significance to the isolation of oil, gas and water layers, and the monitoring of cementing quality is an extremely important part, which greatly guides and promotes the further development of oil and gas. In the process of horizontal well cementing, the lack of cement or the existence of micro-rings will lead to the deterioration of the interlayer isolation effect and wellbore integrity, the reservoir development efficiency will be reduced, and even oil and gas well accidents will occur. The Norwegian Petroleum Safety Authority has conducted a wellbore integrity survey on many oil wells, pointing out the importance of well cementing (Vignes and Aadnoy, 2008).

The comprehensive evaluation of cementing quality is an integral and systematic project (Singh et al., 2012; Khalifeh et al., 2017). Based on acoustic logging (Hawkes and Gardner, 2013), temperature logging, resistivity logging, oxygen activation logging, gamma-gamma density logging, neutron logging (Zemke et al., 2017) et al., many scholars have carried out a lot of very meaningful studies. According to the process of interaction between gamma-ray and the medium, using the density calibration equation to calculate the cement density is a commonly used method. Cocanower et al. (1963) measured the density of the cement in the laboratory and the field, showed that the density measurement method can monitor the absence of cement, low-density cement, etc., thereby demonstrating the sealing ability of cement. Moake (1998) designed a four-detector density logging tool for cased hole detection and obtained the casing thickness, cement density and thickness, and formation density by the gamma-ray measured of the four detectors. Wu et al. (2013, 2017) simulated the response of

* Corresponding author.
*E-mail address:* zhfxy_cn@upc.edu.cn (F. Zhang).

https://doi.org/10.1016/j.petsci.2023.10.007
1995-8226/

the far detector of the density logging tool to the borehole fluid, casing thickness, cement density and formation density under the condition of the cased hole and established the relevant response equation to perform inversion calculations to obtain the casing thickness, cement density and formation density, but this method is not universal. Hu and Guo (2015) processed the energy spectrum recorded by the density logging tool, extracted parameters to evaluate the pore volume and position in the cement. But applying cementing evaluation method in vertical well to horizontal well would lead to inaccuracy in interpretation results (Batcheller, 2013), so it is necessary to establish a new cementing quality monitoring method for horizontal well. In addition, these methods can be used in cementing quality monitoring of vertical wells to calculate cement density, which mainly use gamma-ray counts and cement density to establish a functional relationship, also called calibration equation, to determine the cement density. However, the cement density calculation method by calibration equation does not have azimuthal characteristics and cannot solve the influence of horizontal well casing eccentricity on cement density calculation. Therefore, it is urgent to develop a method for calculating cement azimuthal density in horizontal wells.

This paper adopts a density logging system consisting of a $^{137}Cs$ gamma source, a near detector and six far detectors arranged in a circumferential direction to quantitatively calculate the cement azimuthal density of the horizontal well. The casing eccentricity and cement azimuthal density are regarded as the main factors affecting the gamma-ray counts recorded by the detectors. Using the multi-detector gamma-ray counts of the calibration pit when the cement is well-filled and the casing is centered as the reference condition. Based on the disturbance theory, the Mento Carlo simulation method is used to establish the spatial dynamic response functions for the multi-detector of different casing eccentricities, and the contribution of different azimuthal cement to the multi-detector gamma-ray counts is obtained. A multi-parameter equation system for gamma-ray counts, cement azimuthal density and casing eccentricity measured is established. Using the regularized Newton iteration method, the cement azimuthal density is measured, and the calculation accuracy of cement azimuthal density is improved. The effectiveness of the method is proved by a field example, which provides a new idea for the quantitative evaluation of cementing quality in horizontal well.

## 2. Methodology

The cement density in horizontal well can be evaluated using 0.662 MeV gamma-ray emitted by $^{137}Cs$ gamma source, and the gamma-ray counts detected depend on the scattering and attenuation of photons with the surrounding media, shown in Fig. 1. The quadruple media which interact with photons include the borehole, casing, cement and formation, and the gamma-ray counts can be written as (Priyada et al., 2011):

$$N = N_0 \prod_{i=1}^{4} \mathrm{e}^{-\mu_i \rho_i h_i} S_i \tag{1}$$

where $N$ and $N_0$ are the detected and incident counts of gamma-ray, and $\mu_i$, $\rho_i$ and $h_i$ are the mass attenuation coefficient, density and the equivalent thickness of the quadruple media, respectively. Meanwhile, $S_i$ represents the probability of the photon scattering with the media.

The spatial dynamic response function based on the perturbation theory which reflects the contribution distribution of the surrounding media to the detector, has been successfully applied to the calculation of formation azimuthal density and neutron

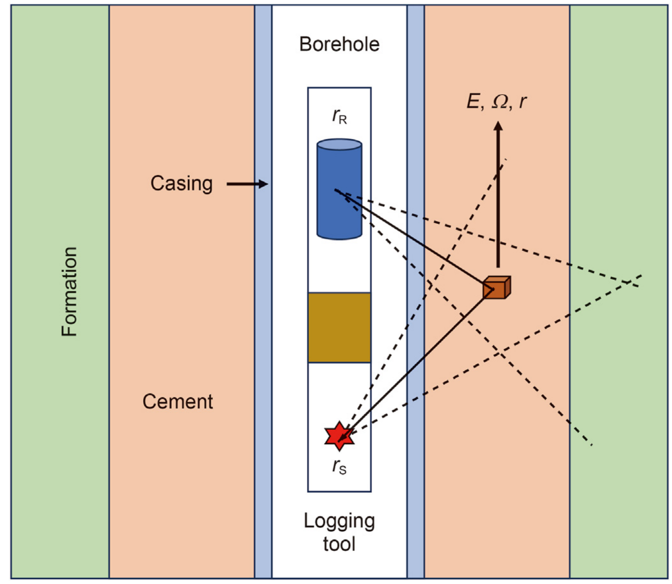


**Fig. 1.** The path of gamma-ray of quadruple media.

porosity. Mendoza et al. (2007) proposed to use the Monte Carlo method to calculate the spatial flux dynamic response function (FSF) and developed a fast approximate numerical program for specific tools, which can be used for neutron porosity logging and density logging. Zhou et al. (2009) extended the density response function to a second-order approximation with improved accuracy and generality compared to linear sensitivity techniques. Mendoza et al. (2009) used the linear approximation of the spatial flux dynamic response function to realize the inversion of density logging while drilling, which improved the interpretation of azimuthal density and reduced the influence of surrounding formation. Therefore, it is an important means to calculate the cement azimuthal density in horizontal well by spatial dynamic response function, which considers the comprehensive influence of casing eccentricity and cement azimuthal density on gamma-ray detection.

Since the attenuation and scattering process of photons in the medium are affected by photon energy, scattering position, and scattering solid angle subtended by the detector, the gamma-ray counts detected at position $r_R$ can be expressed as (Mendoza et al., 2010):

$$N(r_R) = \int \mathrm{d}\boldsymbol{r} \int \mathrm{d}E \int \mathrm{d}\Omega \psi(r_S, r, E, \Omega) S(r_S, r, E, \Omega) \tag{2}$$

where $N(r_R)$ is the gamma-ray counts recorded by the detector, $\psi(r_S, r, E, \Omega)$ represents the gamma-ray counts emitted from the source $r_S$ to the position $r$, $S(r_R, r, E, \Omega)$ represents the probability of the photons reaching the detector position $r_R$ after scattering at position $r$. $\Omega$ is the solid angle subtended by the detector and $E$ is gamma-ray energy.

The gamma-ray counts change with the physical properties of the medium change. Assuming that the change in density at the medium position $r$ is $\Delta\rho(r)$, based on the perturbation theory, the $\Delta N(r_R)$ that is the change in the gamma-ray counts detected can be expressed as:

$$\Delta N(r_R) = \int \mathrm{d}\boldsymbol{r} \int \mathrm{d}E \int \mathrm{d}\Omega \psi(r_S, r, E, \Omega) S(r_S, r, E, \Omega) \times C\left(\frac{\Delta\rho(r)}{\rho(r)}\right) \tag{3}$$

where $\rho(r)$ is the density of the medium and $C\left(\frac{\Delta\rho(r)}{\rho(r)}\right)$ is a function of the relative change in density.

Combining Eqs. (2) and (3), a new expression of the change of the gamma-ray counts can be obtained:

$$\Delta N(r_R) = N(r_R)\int d\boldsymbol{r}\int dE\int d\Omega \frac{1}{N(r_R)}\psi(r_s,r,E,\Omega)S(r_s,r,E,\Omega) \times C\left(\frac{\Delta\rho(r)}{\rho(r)}\right) \tag{4}$$

where $\int d\Omega \frac{1}{N(r_R)}\psi(r_s,r,E,\Omega)S(r_s,r,E,\Omega)$ is the spatial dynamic response function, which represents the degree of influence of medium density changes on gamma-ray counts, and its spatial integral over the entire density variation region is 1.

Based on the density logging system consisting of a $^{137}$Cs gamma source, a near detector and six far detectors arranged in a circumferential direction, in the project of cement azimuthal density monitoring in horizontal well, the gamma-ray counts detected by each detector can be expressed as the gamma-ray counts of the reference condition with the same cement azimuthal density and no casing eccentricity multiplies the convolution of the spatial dynamic response function and the relative change in cement density. The gamma-ray counts can be expressed as:

$$N(r,x)_n = N(r,x)_{\text{ref},n} \times \left(\sum_{i=1}^{m}\omega(i)\right)_n T_{\text{ca}}(x)_n\Delta\rho_{\text{ca}}(i) + T_{\text{f}}(x)_n\Delta\rho_{\text{f}}\Bigg) \tag{5}$$

where $n$ is the number of the detector in the cement azimuthal density measurement system, $m$ is the total number of cement sectors, $N(r,x)$ represents the gamma-ray counts when the casing eccentricity is $x$ and the spacing is $r$, $N(r,x)_{\text{ref}}$ is the gamma-ray counts under the reference condition, and $w(i)$ is the integral of the spatial dynamic response function in the $i$-th cement sector, $T_{\text{ca}}(x)$ and $T(x)$ represent the response between the gamma-ray counts and the density of the entire cement and the formation. $\Delta\rho_{\text{ca}}(i)$ is the difference between the density of the $i$-th cement sector and the reference of cement density, and $\Delta\rho_{\text{f}}$ is the difference between the formation density and the reference of formation density.

Therefore, a set of equations for calculating the cement azimuthal density is established by the gamma-ray counts detected by each detector, shown in Eq. (6):

$$F(\Delta\boldsymbol{\rho}_{\text{ca}},x)_n = 0 \quad n = 1,\ 2,\ 3,\ \ldots,\ 7 \tag{6}$$

Subject to:

$$F(\Delta\boldsymbol{\rho}_{\text{ca}},x)_n = N(r,x)_n - N(r,x)_{\text{ref},n} \times \left(\sum_{i=1}^{m}\omega(i)\right)_n T_{\text{ca}}(x)_n\Delta\rho_{\text{ca}}(i) + T_{\text{f}}(x)_n\Delta\rho_{\text{f}}\Bigg) \tag{7}$$

where $\Delta\boldsymbol{\rho}_{\text{ca}}$ is the cement density difference between each sector and reference condition, and $x$ is the casing eccentricity.

The optimal solution of the above calculation model is obtained by the Newton iteration method. The iterative form is as follows:

$$(\Delta\boldsymbol{\rho}_{\text{ca}},x)^{k+1} = (\Delta\boldsymbol{\rho}_{\text{ca}},x)^{k} - F'\left[(\Delta\boldsymbol{\rho}_{\text{ca}},x)^{k}\right]^{-1} \times F\left[(\Delta\boldsymbol{\rho}_{\text{ca}},x)^{k}\right] k=0,1,2,\ldots \tag{8}$$

For the iterative method, we hope to find an approximate solution, which can be close to the exact solution on the one hand, and the stability in the iterative process should be guaranteed on the other hand. In this paper, the Tikhonov regularization method is used to reconstruct the Jacobian matrix $F'(\Delta\boldsymbol{\rho}_{\text{ca}},x)^k$ in the iterative process, and the number of singular values $k$ is reserved to balance the contradiction between the accuracy of the solution and the iterative stability. The larger the $k$ value, the higher the accuracy, and the smaller the $k$ value, the higher the stability. The optimal solution to the problem is obtained by multiple iterations, the iteration is stopped when the difference in cement density between the two iterations is less than 0.03 g/cm$^3$ and the difference in casing eccentricity is less than 0.2 cm.

Combining the optimal value of $\Delta\boldsymbol{\rho}_{\text{ca}}$ and $x$ and the cement density of reference condition, the cement azimuthal density and the casing eccentricity are obtained. Therefore, this method realizes the cement azimuthal density monitoring in horizontal well cementing, and the negative influence of casing eccentricity on the calculation of cement azimuthal density is eliminated.

## 3. The numerical simulation

### 3.1. The model of formation and instrument

MCNP is a general-purpose Monte Carlo N−Particle code (Team, 2003), which can be used for neutron, photon, electron or coupled neutron/photon/electron transport, with wide application in nuclear and accelerator physics, as well as in medical and space science fields, like particle transport, radiation protection and radiometry, radiation shielding design optimization, and detector design and analysis.

This study applies MCNP to build a numerical model of formation and instrument, as illustrated in Fig. 2. The borehole is filled with fresh water (in 12.5 cm diameter size), the casing is 0.7 cm thick and made with 17-4 PH steel, while the cement is 3 cm thick and made with $CaSiO_3$. The logging tool adopts the $^{137}$Cs as the gamma-ray source, NaI is selected as the detector crystal, and the spacing are 20 cm and 40 cm. The length of near and far detectors is 4 cm and 6 cm, and the diameter of both near and far detectors is 1.58 cm. Shielding is added between the source and the detector to ensure the accuracy of the measured energy spectrum.

It can be seen from the previous analysis that the premise of the cement azimuthal density inversion is to obtain the cement density response and the spatial dynamic response function of different detectors under different casing eccentric conditions. Therefore, we use the MCNP numerical calculation model to establish the density response relationship and the spatial dynamic response function, which lays the foundation for the inversion method of the cement azimuthal density.

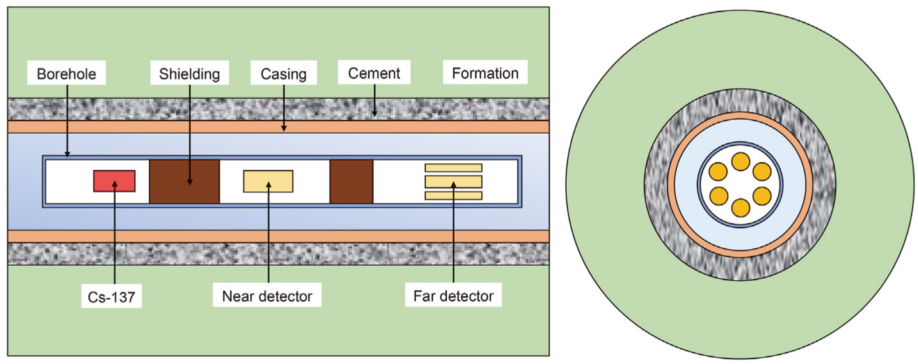


**Fig. 2.** The model of formation and instrument.

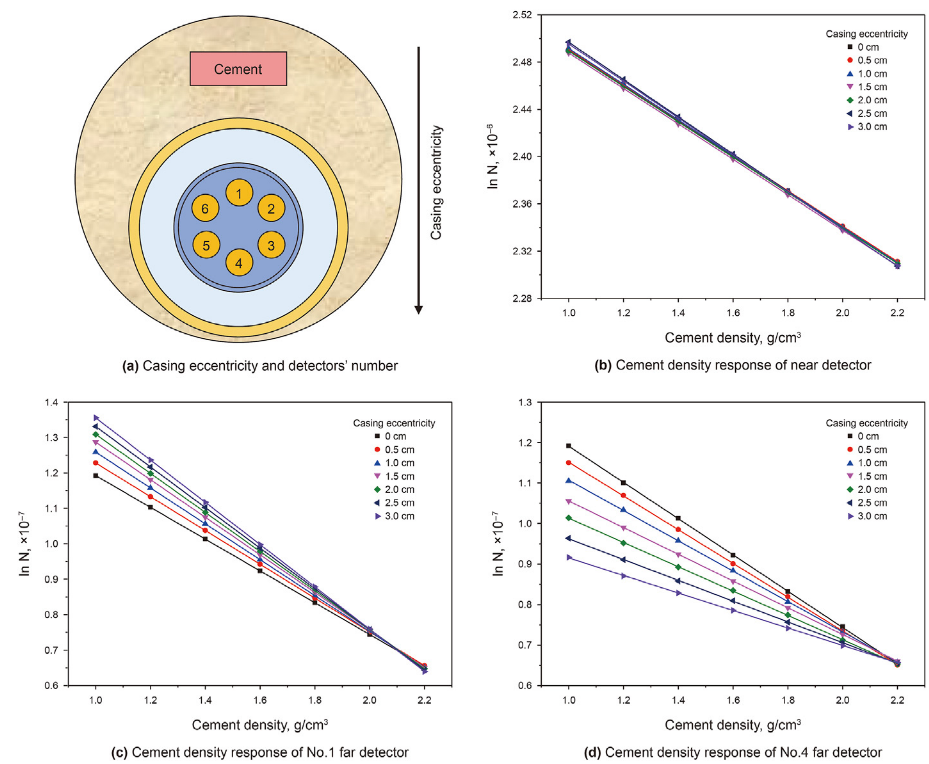


**Fig. 3.** Schematic diagram of the casing eccentricity and the cement density response of different detectors.

### *3.2. Cement density response under casing eccentricity*

Since the monitoring of cement azimuthal density in horizontal well is affected by casing eccentricity, it is basic work to study the gamma-ray counts' response under different conditions of casing eccentricity. We take the casing with no eccentricity as the reference condition. Based on the numerical calculation model shown in Fig. 1, the casing eccentricity is set as 0 cm, 0.5 cm, 1 cm, 1.5 cm, 2 cm, 2.5 cm, and 3 cm, the cement density is changed to 1 g/cm$^3$, 1.2 g/cm$^3$, 1.4 g/cm$^3$, 1.6 g/cm$^3$, 1.8 g/cm$^3$, 2 g/cm$^3$ and 2.2 g/cm$^3$ and the formation is set to sandstone with 10% porosity. Then the relationship between gamma-ray counts and cement density of the near and far detectors under the condition of casing eccentricity are obtained. Fig. 3a is a schematic diagram of the casing eccentricity and the number of the far detectors, and Fig. 3b–d shows the relationship between the gamma-ray counts and cement density of the near detector, No.1 and No.4 far detectors.

The casing eccentricity influences the response relationship of the gamma-ray counts to the cement density. Due to the shallow detection range of the near detector, even if the casing is eccentric, the medium in the detection range and the response between the gamma-ray counts and the cement density remains unchanged. There is a certain difference in the response relationship of the far detector between the gamma-ray counts and the cement density due to the difference in the casing eccentricity. The gamma-ray counts measured by the detector depends on the medium parameters in the detection range. In this paper, six far detectors measure the medium of cement and part of formation, with the increase of casing eccentricity, the contribution of cement increases gradually in the detection range of No.1 far detector. Therefore, for No.1 far detector, the range of cement detected increases with the increase of casing eccentricity, the easier it is to detect changes in cement density, and the sensitivity of the response between the gamma-ray counts and the cement density increases synchronously.

Meanwhile, for No.4 far detector, the range of cement detected decreases with the increase of casing eccentricity, and the sensitivity of the response between the gamma-ray counts and the cement density decrease. Therefore, it can be said that the response relationship between the gamma-ray counts and the cement density is affected by the casing eccentricity, and it must be considered when calculating the cement azimuthal density.

In general, even if the density of the cement changes uniformly, the eccentricity of the casing still affects the response relationship between the gamma-ray counts and the cement density, and the influence is more complex when the density of the cement changes unevenly. Therefore, the casing eccentricity needs to be used as a parameter for joint inversion when establishing the cement azimuthal density calculation method based on multi-detector gamma-ray counts.

### 3.3. The spatial dynamic response function

We note that when inverting the cement azimuthal density, it is necessary to obtain the response relationship of the gamma-ray counts to the cement density $S_{ca}(x)$ and the spatial dynamic response function of cement density $w(\theta_i)$ firstly. Therefore, in addition to the above study of the cement density response of different casing eccentricity conditions, the acquisition of the spatial dynamic response function of cement density and its distribution in different sectors is indispensable. Based on the reference condition and perturbation theory, we change the density of the medium outside the casing and obtain the spatial dynamic response function database by simulation. A total of 49 sets of the distribution of spatial dynamic response functions are included in the database, representing the spatial dynamic response functions of all seven detectors with different casing eccentricities (0–3 cm interval 0.5 cm) under the cement density of 1.89 g/cm$^3$. Fig. 4a–f shows the spatial dynamic response functions of the near detector, the No.1 and the No.4 far detector when the casing is centered or eccentric.

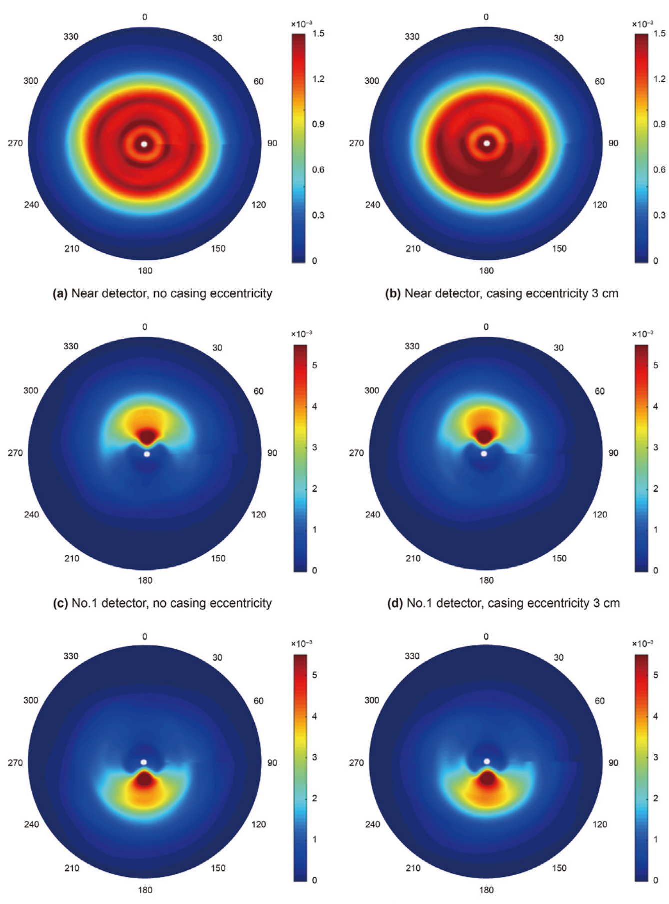


**Fig. 4.** The spatial dynamic response function.

According to the spatial dynamic response function distribution, the gamma-ray counts is most affected by changes in the medium density in the region the detector is directly facing, whether it is a near detector or a far detector. It shows that the spatial dynamic response function distribution does not change much when the casing is centered to eccentric. However, the spatial dynamic response function distribution of the near and far detectors is quite different. The circumferential distribution of the spatial dynamic response function of the near detector is uniform, but for the far detectors, the spatial dynamic response function at the position facing the detector is stronger than other positions. Therefore, based on the influence of the density change of the cement on the gamma-ray counts, the cement is divided into six sectors, and the influence degree of the different cement sector's density change on different gamma detectors can be obtained by integrating the spatial dynamic response function. Fig. 5a is the sector distribution of cement, and Fig. 5b–d shows the influence of the 6-sector cement density change on the gamma-ray counts of the near detector, No. 1 and No. 4 far detectors under different casing eccentricities.

By integrating the spatial dynamic response function, for the near detector, when the casing is centered, the contribution of cement in each sector to the near detector is consistent. With the increase of casing eccentricity, the contribution of different cement sectors to the near detector is gradually reflected. For the far detector, when the casing is centered, due to the circumferential arrangement of the six detectors, the cement sector facing the detector direction has the greatest contribution to the detector. The difference in the contribution of different cement sectors to the gamma-ray counts of the No.1 far detector is small under different casing eccentricities, but it cannot be ignored.

It can be seen from the above forward analysis that the gamma-ray detected not only depends on the eccentricity of the casing but also depends on the cement azimuthal density. Using the response relationship of the gamma-ray counts to cement density of the near and far detectors under different casing eccentricities, combined with the gamma-ray contribution distribution of the cement to multiple detectors obtained by the spatial dynamic response function, it is important to establish cement azimuthal density inversion method in horizontal well.

## 4. Verification of cement azimuthal density inversion method

Newton iteration method is widely used in engineering and exploration technology and solves many problems (Hou and Symes, 2016; Liu et al., 2013; Zhang et al., 2021). This paper adopts the Newton iteration method with the regularization method to obtain the cement azimuthal density in horizontal well and ensure the stability of the cement azimuthal density inversion process simultaneously. Thus, the ambiguity of the cement azimuthal density evaluation in horizontal well cementing evaluation is eliminated.

To verify the effectiveness of this method, we establish several sets of models to calculate the cement azimuthal density. Table 1 shows the cement azimuthal density and casing eccentricity set in the model, Table 2 exhibits the azimuthal density and absolute error of the cement obtained by the inversion method proposed in this paper.

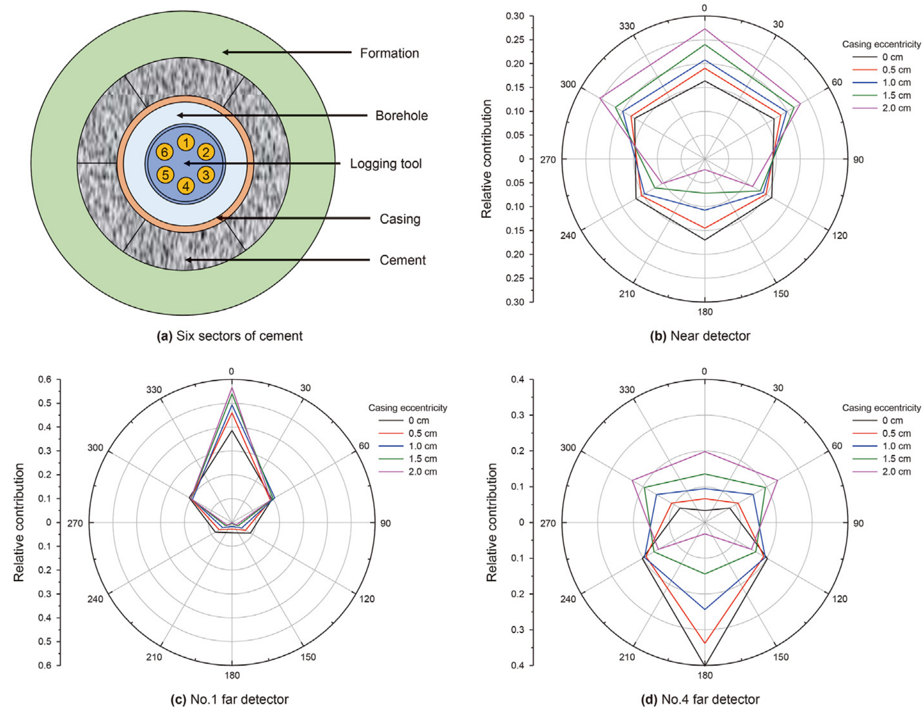


**Fig. 5.** The sector distribution of cement, and the contributions of different cement sectors from the spatial dynamic response function under casing eccentricity.

**Table 1**
The cement azimuthal density set in the models.

| Model number | Casing eccentricity, cm | Cement density, g/cm$^3$ | | | | | |
|---|---|---|---|---|---|---|---|
| | | Sector 1 | Sector 2 | Sector 3 | Sector 4 | Sector 5 | Sector 6 |
| 1 | 0.57 | 1.5 | 1.6 | 1.7 | 1.8 | 1.6 | 1.5 |
| 2 | 0.91 | 1.3 | 1.5 | 1.5 | 1.6 | 1.7 | 1.3 |
| 3 | 2.36 | 1.35 | 1.6 | 1.8 | 1.8 | 1.8 | 1.5 |
| 4 | 1.25 | 1.7 | 1.5 | 1.5 | 1.8 | 1.8 | 1.7 |
| 5 | 1.75 | 1.6 | 1.7 | 1.5 | 1.4 | 1.6 | 1.7 |

**Table 2**
The cement azimuthal density and its absolute error by the inversion method.

| Model number | Cement density, g/cm$^3$, and absolute errors, g/cm$^3$ | | | | | | Average errors, g/cm$^3$ |
|---|---|---|---|---|---|---|---|
| | Sector 1 | Sector 2 | Sector 3 | Sector 4 | Sector 5 | Sector 6 | |
| 1 | 1.465(0.035) | 1.624(0.024) | 1.724(0.024) | 1.840(0.040) | 1.630(0.030) | 1.535(0.035) | 0.031 |
| 2 | 1.351(0.051) | 1.453(0.047) | 1.465(0.035) | 1.637(0.037) | 1.659(0.041) | 1.261(0.039) | 0.041 |
| 3 | 1.329(0.021) | 1.580(0.020) | 1.781(0.019) | 1.813(0.013) | 1.779(0.021) | 1.510(0.010) | 0.017 |
| 4 | 1.676(0.024) | 1.475(0.025) | 1.538(0.038) | 1.769(0.031) | 1.756(0.044) | 1.670(0.030) | 0.032 |
| 5 | 1.585(0.015) | 1.663(0.037) | 1.475(0.025) | 1.367(0.033) | 1.582(0.018) | 1.687(0.013) | 0.023 |

**Table 3**
The cement azimuthal density and its absolute error by the calibration equation.

| Model number | Cement density, g/cm$^3$, and absolute errors, g/cm$^3$ | | | | | | Average errors, g/cm$^3$ |
|---|---|---|---|---|---|---|---|
| | Sector 1 | Sector 2 | Sector 3 | Sector 4 | Sector 5 | Sector 6 | |
| 1 | 1.737(0.237) | 1.151(0.449) | 2.209(0.509) | 1.939(0.139) | 1.824(0.224) | 1.893(0.393) | 0.325 |
| 2 | 1.555(0.255) | 1.694(0.194) | 1.995(0.495) | 1.266(0.334) | 2.004(0.304) | 1.315(0.015) | 0.266 |
| 3 | 1.252(0.098) | 0.957(0.643) | 1.889(0.089) | 2.488(0.688) | 2.252(0.452) | 1.492(0.008) | 0.330 |
| 4 | 1.658(0.042) | 1.600(0.100) | 1.941(0.441) | 2.053(0.253) | 2.333(0.533) | 1.755(0.055) | 0.237 |
| 5 | 1.134(0.466) | 1.837(0.137) | 1.848(0.348) | 1.579(0.179) | 2.284(0.684) | 1.949(0.249) | 0.344 |

The conventional calibration equation is a function of cement density and measured gamma-ray counts from the far detector under the condition of no casing eccentricity and uniform cement distribution. Because of the symmetry of the logging tool and the cement, the gamma-ray counts measured by multiple far detectors are the same. The conventional calibration equation can be expressed as:

$$\rho = A\ln N + B \tag{9}$$

where $\rho$ is the cement density, $N$ is the gamma-ray counts, $A$ and $B$ are the constant coefficients obtained by fitting the gamma-ray counts and cement density.

However, due to the gamma-ray counts detected is determined by both casing eccentricity and cement density in six sectors, the calibration equation cannot truly reflect the cement azimuthal density since the difference of cement azimuthal density and casing eccentricity in the actual cement azimuthal density calculation. Table 3 demonstrates the azimuthal density and absolute error of the cement calculated by using the conventional calibration equation.

From several sets of simulated models, the absolute errors of the cement density inversion calculation are controlled within 0.05 g/cm$^3$, which shows the accuracy of the method. The cement azimuthal density calculated by the conventional calibration equation shows that the absolute errors are quite large, which exceeded 0.3 g/cm$^3$ because the interaction between the multi-azimuthal cement and casing eccentricity on the gamma-ray detection is not considered. Therefore, the inversion method has great advantages in calculating cement azimuthal density in horizontal well cementing due to the casing eccentricity phenomenon, which ensures the calculation accuracy.

## 5. The field logging example

Fig. 6 illustrates the cement azimuthal density interpretation result of 3853–3973 m of Well X. Well X is located in an oil field of Xinjiang, China, and was measured after cementing. The cement density filled during the cementing process was 1.89 g/cm$^3$. Before processing the measured data, we used the Statistics-sensitive Non-linear Iterative Peak-clipping (SNIP) algorithm to eliminate the drastic change of gamma-ray counts curves caused by the casing collar. In the interpretation results, the first track is the depth curve, the second track includes the well inclination curve (DEVI), borehole diameter curve (CALI) and casing collar curve (CCL), the third track is the formation density (DEN_Formation), and the fourth and fifth tracks are the near (N_Near) and far (N1–N6) detector gamma-ray counts curves. The sixth track is the casing eccentricity calculated by the inversion method. Finally, the seventh and eighth tracks are the cement azimuthal density imaging results calculated from the method purposed by this paper and the calibration equation. Using the method of cement azimuthal density calculation proposed in this paper, the azimuthal density imaging result calculated by combining the formation density and the gamma-ray count is obtained, shown in the seventh track, and the eighth track is the cement azimuthal density imaging result

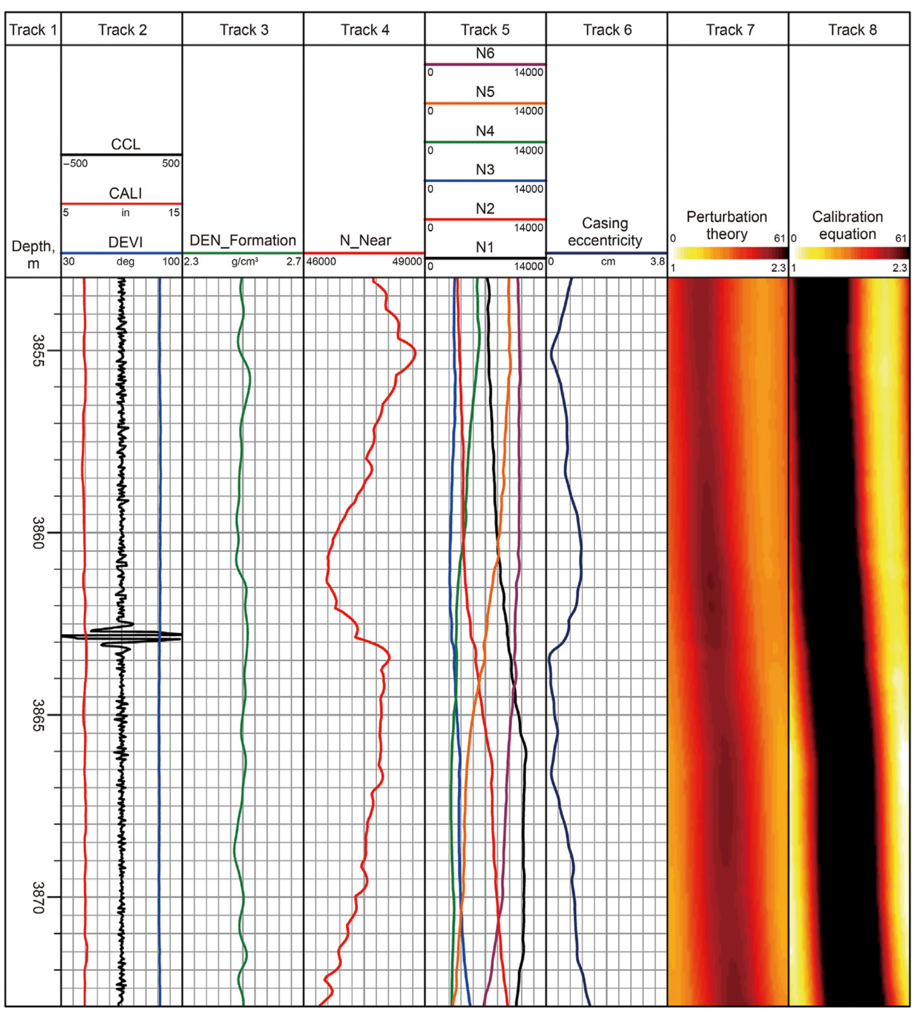


**Fig. 6.** The field logging example.

calculated by the calibration equation.

The gamma-ray counts detected by multiple detectors vary greatly, indicating that there is a certain casing eccentricity in this well section. The interpretation results of casing eccentricity verified this phenomenon. Meanwhile, from the cement azimuthal density imaging map, there is an uneven distribution of azimuthal cement in the well section, which is caused by cement settlement in horizontal well cementing. As mentioned earlier, the interaction between the multi-azimuth cement and casing eccentricity on the gamma-ray detection is not considered in the calibration equation, although the relative size of the cement azimuthal density imaging result shown in track 8 seems to be consistent with track 7, the calculated density range is too large, the highest density is more than 2.5 g/cm$^3$ and the lowest density is less than water density. The density calculation accuracy is low and does not conform to the cognition in actual cementing. Therefore, the inversion method of cement density based on perturbation theory can effectively calculate the cement azimuthal density in horizontal well, which provides a new method for the cement azimuthal density evaluation in horizontal well cementing.

## 6. Conclusion

This paper proposes a novel method for evaluating the cement azimuthal density in horizontal wells. The study analyzes the interactions between gamma-ray and various media such as casing, cement, and formation, elucidating the impact of azimuthal cement on gamma-ray detection. To accurately assess the cement density, the database of spatial dynamic response functions for a multi-detector gamma detection system is established using perturbation theory under different casing eccentricities, which effectively captures the influence of cement density changes on the detected gamma-ray intensity.

By combining the response of gamma-ray counts from multiple detectors with the spatial dynamic response function, a set of inversion equations for determining the cement azimuthal density is derived. The regularized Newton iteration method is then employed to perform the inversion process. This approach considers the casing eccentricity and azimuthal characteristics specific to horizontal wells, resulting in a cement azimuthal density accuracy within 0.05 g/cm$^3$.

The effectiveness of the proposed method is further validated through a field example, highlighting its ability to provide quantitative monitoring of cement azimuthal density in horizontal wells. Overall, this technique offers a reliable and efficient solution for evaluating cement azimuthal density in horizontal well.

## Declaration of competing interest

The authors declare that they have no known competing financial interests or personal relationships that could have appeared to influence the work reported in this paper.

## Acknowledgements

The authors would like to acknowledge the support of the National Natural Science Foundation of China (41974127, 42174147).

## References

Batcheller, G.W., 2013. Cement evaluation challenges in horizontal wells-guidelines for providing meaningful data. SPE Production and Operations Symposium SPE-164513-MS. https://doi.org/10.2118/164513-MS.

Cocanower, R.D., Dillingham, M.E., Reeves, C., 1963. Density Measurements of Cement Sheaths Provide Accurate Evaluation of Oil Well Cementing Operations. Fall Meeting of the Society of Petroleum Engineers of AIME, SPE-633-MS. https://doi.org/10.2118/633-MS.

Hawkes, C.D., Gardner, C., 2013. Pressure transient testing for assessment of wellbore integrity in the IEAGHG Weyburn–Midale CO2 monitoring and storage project. Int. J. Greenh. Gas Control 16, S50–S61. https://doi.org/10.1016/j.ijggc.2012.12.022.

Hou, J., Symes, W., 2016. Approximate Gauss-Newton iteration for full-waveform inversion. SEG Tech. Progr. Expand. Abstr, 1163–1168. https://doi.org/10.1190/segam2016-13878327.1.

Hu, Y., Guo, W., 2015. Behind-casing cement void volumetric evaluation. SPE. SPE-178447-MS. https://doi.org/10.2118/178447-MS.

Khalifeh, M., Gardner, D., Haddad, M.Y., 2017. Technology trends in cement job evaluation using logging tools. SPE, SPE-188274-MS. https://doi.org/10.2118/188274-MS.

Liu, L., Liu, H., Liu, Y., 2013. Waveform Inversion with Modified Quasi-Newton Algorithm. SEG, SEG-2013-0153. https://doi.org/10.1190/segam2013-0153.1

Mendoza, A., Torres-Verdín, C., Preeg, B., et al., 2009. Inversion of Sector-Based LWD Density Measurements Acquired in Laminated Sequences Penetrated by High Angle and Horizontal Wells. SPWLA, SPWLA-2009-13447.

Mendoza, A., Torres-Verdín, C., Preeg, W., 2007. Rapid Simulation of Borehole Nuclear Measurements with Approximate Spatial Flux-Scattering Functions. SPWLA. SPWLA-2007-O.

Mendoza, A., Torres-Verdín, C., Preeg, B., 2010. Linear iterative refinement method for the rapid simulation of borehole nuclear measurements: Part 2—high-angle and horizontal wells. Geophys 75 (2), E79–E90. https://doi.org/10.1190/1.3335953.

Moake, G.L., 1998. Design of a Cased-Hole-Density Logging Tool Using Laboratory Measurements. SPE, SPE-49226-MS. https://doi.org/10.2118/49226-MS.

Priyada, P., Margret, M., Ramar, R., et al., 2011. Intercomparison of gamma scattering, gammatography, and radiography techniques for mild steel nonuniform corrosion detection. Rev. Sci. Instrum. 82, 035115. https://doi.org/10.1063/1.3562893.

Singh, S.K., Subekti, H., Al-Asmakh, M., et al., 2012. Qatar. An Integrated Approach to Well Integrity Evaluation via Reliability Assessment of Well Integrity Tools and Methods: Results from Dukhan Field. SPE, SPE-156052-MS. https://doi.org/10.2118/156052-MS.

Team, X.-M.C., 2003. MCNP—A General Monte Carlo N-Particle Transport Code, Version 5. National Laboratory Los Alamos, LA-UR-03-1987.

Vignes, B., Aadnoy, B.S., 2008. Well-integrity Issues Offshore Norway. SPE, SPE-112535-PA. https://doi.org/10.2118/112535-PA.

Wu, W., Chen, B., Yu, G., et al., 2017. Responses and data inversion of four-detector scattered-gamma-ray logging in cased holes. J. Pet. Sci. Eng. 159, 691–701. https://doi.org/10.1016/j.petrol.2017.10.001.

Wu, W., Fu, Y., Niu, W., 2013. Numerical simulation of responses for cased-hole density logging. J. Geophys. Eng. 10 (5), 054006. https://doi.org/10.1088/1742-2132/10/5/054006.

Zemke, K., Liebscher, A., Möller, F., 2017. Monitoring of well integrity by magnetic imaging defectoscopy (MID) at the Ketzin pilot site, Germany. Energy Proc. 125, 535–542. https://doi.org/10.1016/j.egypro.2017.08.183.

Zhang, F., Fan, J., Liu, Y., et al., 2021. A new algorithm for evaluating reservoir density based on X-ray logging technology. Appl. Radiat. Isot. 175, 109793. https://doi.org/10.1016/j.apradiso.2021.109793.

Zhou, T., Miles, J., Case, C., et al., 2009. In: A Second-Order Fast-Forward Model for a Gamma-Gamma Density Logging Tool SPE, SPE-124193-MS. https://doi.org/10.2118/124193-MS.